A NOVEL OPTIMIZATION BASED DESIGN METHOD FOR CENTRIFUGAL FANS

K. Bamberger - T. Carolus

Institute for Fluid- and Thermodynamics, University of Siegen, Germany
konrad.bamberger@uni-siegen.de

ABSTRACT

A novel design method for impellers of centrifugal fans with backward curved blades is proposed. The overall geometry of the impellers considered is kept close to customary industrial designs (e.g. circular arc blades). The design method is based on seven simple correlations which determine the geometrical impeller parameters as a function of the targeted aerodynamic duty (design) point. Unlike classic design methods, these correlations are derived from aerodynamic optimization. The objective function of the optimization is the maximization of total-to-static efficiency while precisely matching the targeted design points. The range of design points studied covers the full typical realm of centrifugal fans according to Cordier's diagram. A comparison to the classic slip theory as e.g. by Pfleiderer reveals that the novel method is superior regarding both fulfillment of the targeted design point and energy efficient performance.

KEYWORDS

centrifugal fan, design method, optimization, slip theory

NOMENCLATURE

Latin symbols

D	diameter, m
P	power
Q	flow rate, m³/s
S	blade thickness, m
c	velocity, m/s
h	(blade) width, m
k_i	constants in the design correlations
l	length, m
n	rotational speed, s^{-1}
p	pressure
r	radius
s	tip gap
z	number of blades

Greek symbols

β	blade or flow angle, degrees
δ	specific diameter (nondimensional)
η	efficiency (nondimensional)
φ	flow coefficient (nondimensional)
μ	slip factor (nondimensional)
ρ	density, kg/m³
σ	specific speed (nondimensional)
ω	angular velocity (nondimensional)
ψ	pressure coefficient (nondimensional)

Subscripts

1	upstream of the fan
2	downstream of the fan
dyn	dynamic
m	meridional
t	total
ts	total-to-static
tt	total-to-total
θ	circumferential

Abbreviations

ANN	artificial neuronal network
CFD	computational fluid dynamics
DoE	design of experiment
LMN	local model networks
MLP	multi-layer perceptrons
RANS	Reynolds averaged Navier Stokes

INTRODUCTION

This paper deals with the aerodynamic design of impellers for centrifugal fans, Figure 1. A good aerodynamic design method reliably yields the geometry of a new fan that fulfills the targeted performance in terms of pressure rise Δp and volume flow rate Q with high energy efficiency.

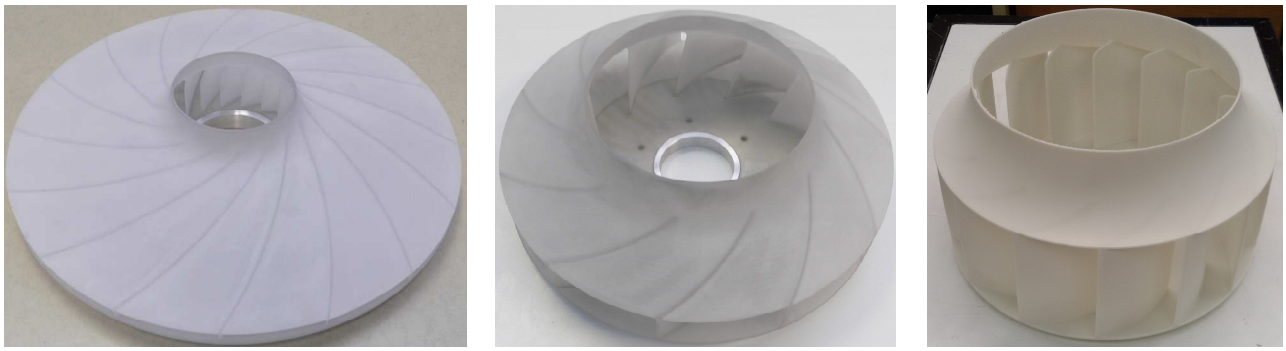

Figure 1: Examples of centrifugal fan impellers for different design points

Q and Δp are the so called design point. Δp can be either total-to-total (Δp_{tt}) or total-to-static (Δp_{ts}). The total-to-total pressure rise is the difference of total pressure downstream (p_{t2}) and upstream of the fan (p_{t1}):

$$\Delta p_{tt} = p_{t,2} - p_{t,1} \tag{1}$$

All common design methods of fans use this pressure rise definition to specify the design point. In many applications (e.g. rotor only fans), however, the dynamic pressure at the fan outlet ($p_{dyn,2}$) is useless as it dissipates in the surroundings. In that case, the total-to-static pressure rise becomes relevant:

$$\Delta p_{ts} = p_2 - p_{t,1} = \Delta p_{tt} - p_{dyn,2} \tag{2}$$

Assuming that the inflow is free of swirl, Δp_{tt} can be computed by Equation (3):

$$\Delta p_{tt} = \eta_{blade} \cdot \rho \cdot \omega \frac{D_2}{2} \cdot c_{\theta 2} \tag{3}$$

η_{blade} is the hydraulic efficiency between inlet and outlet, ρ the fluid density, $\omega = 2\pi n$ the angular velocity of the impeller and $c_{\theta 2}$ the circumferential velocity of the flow at the impeller outlet. The outer impeller diameter D_2 and rotational speed n are the main machine parameters and are assumed to be given at the beginning of a design process. Hence, the main challenge of the designer is to estimate η_{blade} and to find an impeller geometry which yields the $c_{\theta 2}$ which is required to produce Δp_{tt}. Starting in the early 1900's, successful methods for linking $c_{\theta 2}$ to the impeller geometry have been developed by Pfleiderer [1, 2], and later by Eck [3] as well as many others. In essence it is the underperformance factor

$$\mu = \frac{\Delta p_{tt}}{\Delta p_{tt,th}} \tag{4a}$$

which links the actual to the theoretical pressure rise for blade-congruent flow. Pfleiderer' approach [2] for instance is

$$\mu = \left(1 + \frac{k \cdot \left(1 + \frac{\beta_{b2}}{60°} \right)}{z \left(1 - \left(D_1 / D_2 \right)^2 \right)} \right)^{-1} \tag{4b}$$

where the factor k is usually between 1.2 and 2. From (3) and (4a, b) it is possible to compute $\Delta p_{tt,th}$ and the corresponding theoretical circumferential velocity $c_{\theta 2,th}$ which eventually yields the blade outlet angle required to achieve the desired pressure rise. Obviously μ depends on the blade outlet angle β_{b2}, which in turn depends on the underperformance factor. Hence Pfleiderer's approach requires an iterative determination of μ. A user-friendly summary of these methods is given by Carolus [4]. Moreover, Carolus summarizes recommendations by Bommes [5] and Pohl [6] to determine adequate values of the other geometrical parameters, e.g. the blade widths h_1 and h_2 and the inner diameter D_1. Those recommendations are supposed to lead to reasonably good designs with an acceptable impeller efficiency defined as

$$\eta = \frac{Q \cdot \Delta p}{P_{shaft}} \tag{5}$$

where P_{shaft} is the shaft power driving the impeller. In general, the resulting efficiency of a fan can be computed with both Δp_{tt} and Δp_{ts} yielding the total-to-total-efficiency η_{tt} or the total-to-static-efficiency η_{ts}, respectively. In all common design methods, however, the focus is on η_{tt}. The aforementioned design methods have the advantage of being applicable to a wide range of design points and that they require nearly no computational resources. The main drawback lies in the inherently empirical base (indicated for instance in the considerable scatter in the coefficient of approach (4b) from 1.2 to 2.0) which limits the reliability of the method regarding the fulfillment of the design point. Moreover, the maximum achievable efficiency may not be achieved.

More recently Computational Fluid Dynamics (CFD) is coupled with optimization algorithms. A typical example (among many others) is the work by Lee et al. [7] who used CFD-based optimization to reduce the shaft power of a centrifugal fan by 9 %. While CFD-based optimization can yield a highly efficient design of a specific machine, it suffers from long computing times. Hence, the latest technique is to substitute CFD by CFD-trained metamodels (e.g. artificial neural networks, ANN). The effectiveness of this approach is generally acknowledged and even applied commercially, see e.g. [8-10]. However, the computational cost is still significant due to the necessity to generate a CFD-database required to train the ANNs.

The aim of this work is to develop a novel design method which can be applied similarly as the classic methods, i.e. a design point is given and the corresponding geometrical parameters of the impeller are computed analytically. By contrast with the classical method the semi-empirical equations are replaced by correlations that essentially stem from aerodynamic optimization with a generalized metamodel for the complete class of typical radial fans. The metamodel is obtained one time only prior to any individual design task by a comprehensive CFD-study (as reported in [11] by the authors of this paper). This novel design method aims at yielding fan impeller geometries within the full class of centrifugal fans that fulfill more reliably the targeted design point - with the highest efficiency possible.

OPTIMIZATION SCHEME

Initially, the geometry of the impeller needs to be parameterized. Those parameters are then varied by Design of Experiment (DoE) and CFD simulations are performed for each geometry variation. The resulting CFD dataset is then used for training artificial neural networks which are eventually coupled with an evolutionary optimization algorithm. In the subsequent section this optimization scheme is applied for deriving the desired design correlations.

Parameterization

Since the design correlations shall be generally applicable, all correlated quantities are non-dimensional. Lengths are non-dimensionalized with the outer fan diameter D_2 and all velocities are non-dimensionalized with the circumferential blade velocity ωr_2 yielding a velocity coefficient φ_c. The design point is non-dimensionalized as usual in turbomachinery literature (see e.g. [12]) yielding the flow and the pressure coefficient

$$\varphi = \frac{Q}{\frac{\pi^2}{4} D_2^3 n}, \quad \psi = \frac{\Delta p}{\frac{\pi^2}{2} D_2^2 n^2 \rho}. \tag{6a, b}$$

The main objective of the impeller parameterization is to enable a high level of geometrical flexibility while keeping the number of free geometry parameters to a minimum. For that reason, basic parameters which are also used in classic literature [2, 5] are selected. Those parameters are graphically illustrated in Figure 2 and listed in Table 1. The blades have a circular arc shape between the inner diameter D_1 and the outer diameter D_2. The hub is a flat disc perpendicular to the

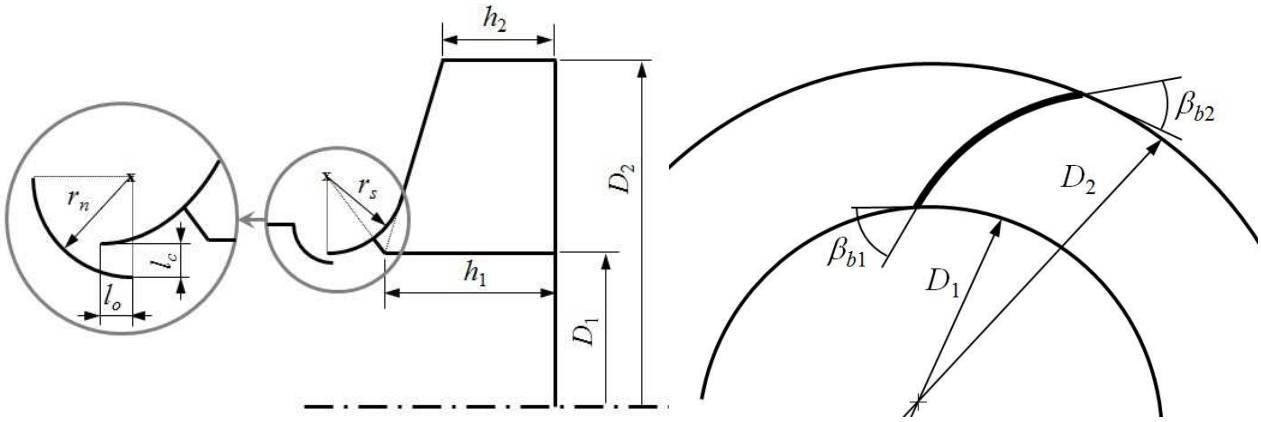

Figure 2: Graphical illustration of the geometrical parameters in side and top view

Table 1: Independent geometrical parameters

Description	Symbol/ Definition	Min. Value	Max. Value
Number of blades[1]	z	5	16
Diameter ratio	D_1/D_2	0.25	0.8
Inlet blade angle	β_{b1}	20°	60°
Inlet blade angle	β_{b2}	20°	60°
Inlet blade width[2]	h_1/D_2	0.025	0.4
Outlet blade width[2]	h_2/D_2	0.025	0.4
Shroud radius	r_s/D_1	0.14	0.3

[1] only integers are possible
[2] h_2 must be smaller than or equal to h_1

Table 2: Dependent and constant geometrical parameters

Description	Symbol/ Definition	Value
Outer diameter	D_2	0.3 m
Rotational speed	n	50 s^{-1}
Fluid density	ρ	1.2 kg/m^3
Nozzle radius	r_n/D_1	0.25
Clearance	l_c/D_1	0.02
Overlap	l_o/D_1	0.03

axis of rotation. The shroud is not parallel to the hub but tapers between D_1 and D_2. The innermost part of the shroud has a circular shape with the radius r_s. The outer (mostly much larger) part of the shroud has a linear shape determined by the blade widths h_1 and h_2. The blade thickness S is constant. The radius and the center point of the circular blade arc are given via the inlet angle β_{b1} and the outlet angle β_{b2} which are measured between the circumferential direction and a tangent at the blade leading or trailing edge, respectively. There is a small cut-back of the blade in the area where the leading edge touches the shroud. The cutting edge starts at the radius $D_1/2$ at the distance h_1 from the bottom disc and perpendicularly intersects the circular part of the shroud. Together with the number of blades z, this set of parameters represents simple yet widely used impeller geometries which can be manufactured employing cost-efficient techniques. In the context of this study the number of parameters is reasonably low to allow for a systematic variation by design of experiments. D_2 and S are excluded from the design of experiment. D_2 is held constant because we consider the dimensionless aerodynamic performance which is independent of D_2. This also applies to the rotational speed n and the fluid density ρ which are held constant, too. Hence, strictly spoken all results in this study are only valid for one value of a characteristic Reynolds number. The reason why S is no independent parameter is that the blade thickness only has a minor effect on the aerodynamic performance and is usually selected for structural reasons. We here assume that the blade thickness increases with increasing ratio D_1/ D_2 as

$$\frac{S}{D_2} = 0.006 \cdot \frac{D_1}{D_2}. \tag{7}$$

Further geometrical parameters are required to describe the inflow nozzle. Since the inflow nozzle is less relevant with respect to the aerodynamic performance, those parameters are a function of the impeller parameters and do not need to be varied by design of experiments. The inflow nozzle has a simple geometry and is fully described by its outflow diameter and the radius r_n. Between the nozzle and the impeller there is a clearance of the size l_c. The overlap of the nozzle with the fan is l_o. All dependent parameters are listed in Table 2.

Design of Experiment (DoE)

As recommended by Santner et al. [13], a space filling DoE should be chosen, if no prior knowledge about the process is available. Due to its advantages and simplicity [13] a latin hypercube (LH) design has been used. The non-collapsing property of LH designs is one advantage compared to commonly used grid designs. In order to achieve good space filling properties the LH design was optimized with the extended deterministic local search method described by Ebert et al. [14]. Approximately 2000 different impeller geometries were simulated with that DoE and used to train preliminary metamodels. In a second DoE, 2000 additional geometries were defined and simulated. The geometry selection for those 2000 impellers followed two basic ideas: (i) Avoidance of irrelevant sections of the input space (which are aerodynamically suboptimal), (ii) Avoidance of the simulation of geometries which are unlikely to enhance to metamodels (areas of the input space where the aerodynamic performance is almost a linear function of the geometrical parameters and hence easy to model).

CFD Model

The CFD model used for this work emulates a typical experimental set-up of an impeller in a chamber test rig, i.e. the inflow is assumed to traverse a chamber and the inflow nozzle whereas the outflow area is free of obstacles. Figure 3 depicts a sketch of all components considered for the CFD-model. The boundary conditions are constant mass flow rate at the inlet, ambient pressure at the opening and no slip at the walls. Hub, shroud and blade are modeled as rotating walls with the

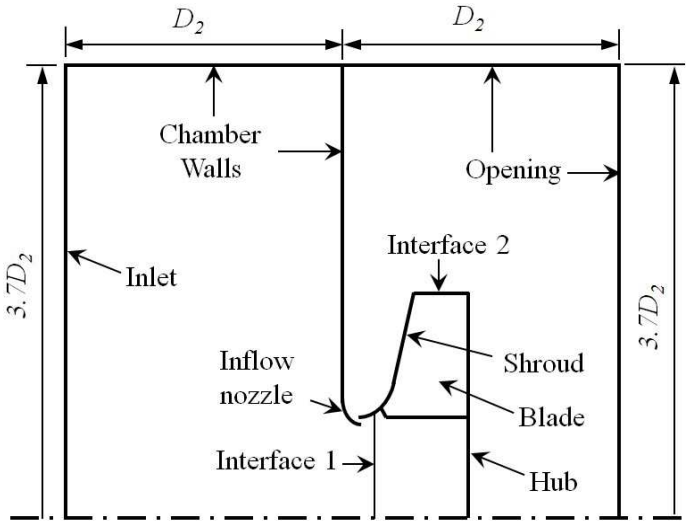

Figure 3: CFD model

rotational speed n whereas all other walls are stationary. Due to the high number of CFD simulations required to train the metamodels, only stationary simulations were affordable, i.e. the Reynolds-Averaged Navier-Stokes (RANS) method was used. The solver selected was ANSYS CFX™ 14.5.7 and the turbulence model used was shear stress transport (SST). As usual in RANS simulations, only one blade channel was simulated and rotational periodicity was assumed at the lateral boundaries. The interface type between the rotating blade and the stationary environment was frozen rotor. In order to determine the fan performance, the quantities Δp_{ts}, Δp_{tt} and P_{shaft} must be extracted from the CFD results. Δp_{ts} is the difference between the area-averaged pressure at the opening and the inlet. The dynamic pressure required to determine Δp_{tt} is evaluated at the interface between the impeller outlet and the environment. The overall shaft power P_{shaft} equals the sum of the powers associated with all rotating surfaces, i.e. the surfaces at the blade, the hub and the shroud. The computational grid of the impeller was generated with ANSYS TurboGrid™ 14.5.7 and the grid of the environment was generated with ICEM CFD™. A grid optimization was performed to find the best compromise between accuracy and computational time. Details about this grid optimization and an experimental validation of the CFD model are discussed in [11].

Metamodel Training

Two meta-model types were tested: Local Model Networks (LMN) and Multi-Layer Perceptrons (MLP). LMNs follow a divide-and-conquer strategy. The input space spanned by all geometry parameters is divided into small sub-spaces, where simple local models are able to sufficiently well describe a part of the whole function to be approximated. For the training of the LMNs the hierarchical local model tree (HILOMOT) algorithm (see Nelles [15]) was used with local linear models. The structure of the LMN grows incrementally by adding a further division of one pre-existing sub-space. Therefore, one local model is added in each step until a termination condition is met. For the automatic prevention of overfitting the available data can be split into two datasets for training and validation. An increase of the validation error indicates beginning overfitting. For the termination of the LMN training process 20% of the available data was utilized as validation data. As soon as the validation error increased two times in succession, the training was terminated in order to prevent the model from overfitting.

MLPs consist of the input layer, one or more hidden layer(s) and the output layer. The number of hidden layers and the number of neurons in each of the hidden layers determines the complexity of the model. In the present work, two hidden layers were used and the number of neurons in each hidden layer was optimized aiming at a minimal validation error. Training an MLP for a given

structure means optimization of the weights in the hidden layers. This was performed with the Neural Network Toolbox of Matlab™ which uses the Levenberg-Marquardt [16] method. The target function of the weight optimization was the mean squared difference between the MLP output and the CFD results. 80% of the available CFD data was used for that purpose whereas the remaining 20% was used for validation. It was found that the MLPs performs slightly better than the LMNs, but that the most reliable prediction is obtained when using both models and averaging the respective outputs (weighted with the inverse validation error).

Optimization Algorithm: An evolutionary optimization algorithm was used. The implementation mainly follows the suggestions by Thévenin and Janiga [17]. The basic settings are 2.000 individuals per generation, reproduction via cross-over (80% probability) or averaging (20% probability) and random mutations at the end of each reproduction process. The objective function is maximization of total-to-static efficiency with a penalty term for the violation of the targeted pressure coefficient $\psi_{tt,target}$:

$$\eta^* = \eta_{ts} - \left|\psi_{tt} - \psi_{tt,target}\right| \tag{8}$$

ψ_{tt} and η_{ts} are evaluated by the metamodels. Due to the extremely efficient metamodels the performance of one generation can be computed in less than one second on one CPU of a standard personal computer.

THE NEW CENTRIFUGAL IMPELLER DESIGN METHOD

Step 1 (Heuristic Determination of the Structure of the Design Correlations)

The optimization tool described above was applied for finding the optimal impeller geometries for the 94 design points illustrated in Figure 4. The design points are computed by

$$\psi_{tt,target} = 1 - \frac{1}{0.35}\varphi + \Delta \tag{9}$$

where φ is varied in ten equidistant steps between 0.04 and 0.25 and Δ is varied in ten equidistant steps between -0.3 and +0.3. This initially leads to 100 design points. Due to the constraint $\psi_{tt,target} \geq 0.25$, however, the overall number of different design points reduces to 94. The optimal geometries were examined heuristically to find general correlations about the optimal choice of the geometrical parameters. These correlations are described in the following. As mentioned previously, the correlations shall be as simple as possible. Often, it was easier to define correlations for flow quantities from which the geometrical parameters are derived instead of directly defining correlations for the respective parameters. Most of the following correlations contain one or more

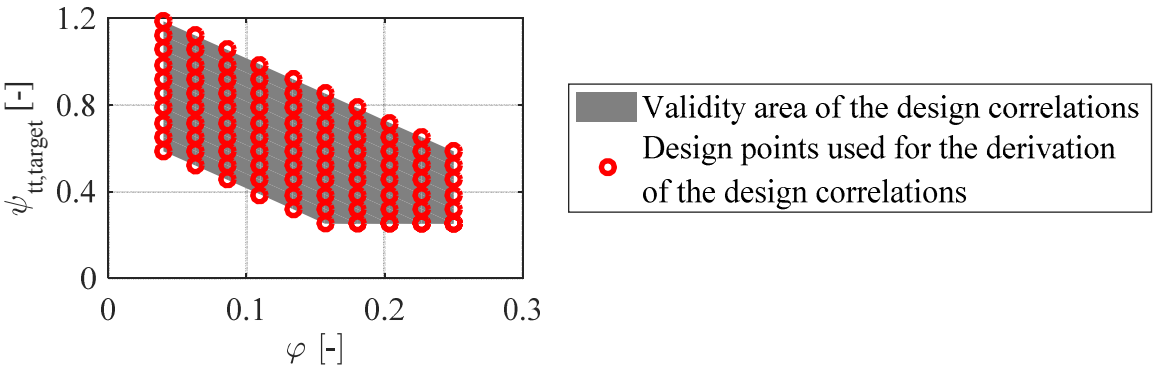

Figure 4: Design points used for the derivation of the design correlations

so far unknown constants k_i. The values of the constants will be identified by subsequent optimization in the second step.

The first design correlation is rather simple. All 94 optimizations yield blade inlet angles which are as flat as possible within the limits defined in Table 1. Therefore

$$\beta_{b,1} \overset{!}{=} 20° . \tag{10}$$

Most probably, the actual optimum is even lower, but this cannot be examined with the existing metamodel which is only valid within the limits defined in Table 1. A constant inlet angle irrespective of the design point is not intuitive. Normally, the angle increases with the flow coefficient to minimize incidence losses. The design target of maximum total-to-static efficiency, however, leads to large throughflow areas to decrease exit losses and consequently to flat inlet angles for all design points. The inlet area is determined by the inner diameter D_1 and the inlet width h_1. These geometrical parameters are basically determined by the second and third design correlation. However, these design correlations do not directly yield the geometrical parameters but the dimensionless meridional inflow velocity φ_{cm1} and the incidence angle $\Delta\beta_1$ from which D_1 and h_1 can be derived via Eq. 17 and 18. φ_{cm1} is always on a similar level and can be approximated by a constant:

$$\varphi_{cm1} = \frac{c_{m1}}{\omega r_1} \overset{!}{=} k_1 \tag{11}$$

The incidence angle $\Delta\beta_1$ (i.e. the difference between the blade angle and the flow angle) is negative at small flow coefficients and asymptotically approaches a shock-free inflow (i.e. $\Delta\beta_1 = 0$) with increasing flow coefficient. This can be expressed via the third design correlation:

$$\Delta\beta_1 = \beta_{b,1} - \beta_1 \overset{!}{=} k_2 \cdot e^{-k_3 \cdot \varphi} \tag{12}$$

Given these three correlations, the inlet geometry is described unambiguously. The next two design correlations are required to describe the outlet geometry. As with the inlet geometry, the outlet design correlations yield flow quantities from which the corresponding geometrical parameters can be derived by Eq. 17 and 18. The fourth design correlation defines the optimal meridional deceleration which is found to be a function of the flow coefficient but independent of the pressure coefficient:

$$\frac{\varphi_{cm2}}{\varphi_{cm1}} \overset{!}{=} k_4 \cdot \varphi^2 + k_5 \cdot \varphi + k_6 \tag{13}$$

The fifth design correlation deals with the underperformance factor μ, i.e. with the quotient of the actually achieved pressure coefficient $\psi_{tt,actual}$ and the theoretical pressure coefficient $\psi_{tt,th}$ that would ensue if the relative exit flow direction was congruent with the blade. Precise prediction of the underperformance factor is of fundamental importance since it is decisive for the accuracy with which the targeted design point is met. One possibility to achieve an accurate prediction is defining a very complex design correlation with many free constants k_i. This strategy, however, would counteract the objective to keep the design correlations as simple as possible. As a consequence, it is suggested to firstly approximate a preliminary underperformance factor by a linear function of φ and $\psi_{tt,target}$. This underperformance factor is then applied to design a preliminary impeller and the

actual pressure coefficient is determined for that machine. In case of unsatisfactory results, the underperformance factor can be corrected:

$$\mu_{prelim} \overset{!}{=} k_7 \cdot \varphi + k_8 \cdot \psi_{tt,target} + k_9$$
$$\mu = \mu_{prelim} \cdot \frac{\psi_{tt,target}}{\psi_{tt,actual}} \tag{14}$$

During the development of the design correlations, $\psi_{tt,actual}$ was determined by the metamodels. In the application of the design correlations, it is assumed that the user determines $\psi_{tt,actual}$ via CFD simulations or experiments. This extra-effort is considered acceptable since in most practical applications corrections are required anyway due to different gaps or inflow conditions as compared to the assumptions used in this study. If the correction is not affordable, the preliminary underperformance factor still will lead to a very acceptable performance.

The sixth and seventh design correlation directly determine geometrical parameters, namely the number of blades z and the radius of the cover disc nozzle r_n. Both parameters are linear functions of φ and $\psi_{tt,target}$. Note that z always needs to be rounded to an integer.

$$z \overset{!}{=} k_{10} \cdot \varphi + k_{11} \cdot \psi_{tt,target} + k_{12}\,, \quad \frac{r_n}{D_2} \overset{!}{=} k_{13} \cdot \varphi + k_{14} \cdot \psi_{tt,target} + k_{15} \tag{15, 16}$$

Since many of the design correlations deal with flow quantities, Equations 17 to 20 are required to determine the corresponding geometrical parameters.

$$\frac{D_1}{D_2} = \frac{\varphi_{cm1}}{tan\left(\beta_{b,1} + \Delta\beta_1\right)}, \quad \frac{b_1}{D_2} = \frac{\varphi}{4 \cdot \varphi_{cm1} \cdot \frac{D_1}{D_2}} \tag{17, 18}$$

$$\frac{b_2}{D_2} = \frac{b_1}{D_2} \cdot \frac{D_1}{D_2} \cdot \left(\frac{\varphi_{cm2}}{\varphi_{cm1}}\right)^{-1}, \quad \beta_{b,2} = a\,tan\left(\frac{\varphi_{cm1} \cdot \frac{\varphi_{cm2}}{\varphi_{cm1}}}{1 - \frac{\psi_{tt,target}}{2 \cdot \mu}}\right) \tag{19, 20}$$

Throughout the development of the design correlations, it was assumed that the limits according to Table 1 must not be exceeded. In case that any of the design correlations leads to parameter values below or above the ranges defined in Table 1, the lower or upper limit must be used, respectively.

Step 2 (Identification of the Constants in the Design Correlations)

The values of the constants k_i are found with the Simplex method by Nelder and Mead [18]. The objective function is maximization of the averaged total-to-static efficiency of the 94 aforementioned design points with penalty terms for the violation of the design points. The resulting optimal values of the constants are summarized in Table 3**.**

Table 1: Optimal constants for the design correlations

Constant	Value	Constant	Value	Constant	Value	Constant	Value	Constant	Value
k_1	0,296	k_4	-0,012	k_7	-0,225	k_{10}	93,2	k_{13}	0,233
k_2	27,3	k_5	0,541	k_8	0,498	k_{11}	26,9	k_{14}	0,453
k_3	12,6	k_6	0,599	k_9	0,238	k_{12}	-19,1	k_{15}	0,04

RESULTS

The full geometry of impellers for the aforementioned 94 design points was identified by means of the design correlations. Subsequently, their actual aerodynamic performance was simulated by means of independent CFD to assess the quality of the design correlations. The first question is how precisely the actual pressure coefficient $\psi_{tt,acutal}$ matches the targeted pressure coefficient $\psi_{tt,target}$. Figure 5(a) illustrates the deviation $\Delta\psi_{tt} = \psi_{tt,actual} - \psi_{tt,target}$. At most design points, the deviation $\Delta\psi_{tt}$ is close to zero. Only at very low targeted pressure coefficients ($\psi_{tt,target} \approx 0.25$) the deviation reaches values of up to 0.04. That means that the actual pressure coefficient $\psi_{tt,acutal}$ of nearly all designs investigated matches the targeted pressure coefficient $\psi_{tt,target}$ very well, or, with other words, the novel design correlations seem to be quite reliable.

The second question is concerned with the efficiency of the various designs. The total-to-static efficiency η_{ts} associated with all designs is depicted in Figure 5(b). At almost all design points, it is around 60 % or moderately higher. The lowest value is obtained at design points with high flow coefficient but low pressure coefficient and amounts to approximately 45 %. Such design targets are more typical for axial fans. Figure 6 depicts the difference between the efficiencies obtained with impellers designed by the novel design correlations and the classic Pfleiderer method. Obviously, the novel design method yields impellers with better performance regarding both total-to-static and total-to-total efficiency. The differences can be as high as 10 percentage points at design points with high targeted pressure coefficients. This observation is in full agreement with an earlier similar study on axial fans [19] which revealed that the potential for improvement through optimization increases with increasing blade loading. Remarkably, the new design method enhances the total-to-total efficiency even more than total-to-static efficiency although the objective function of the optimization algorithm was to maximize total-to-static efficiency. The reason for that is the self-imposed constraint $\beta_{b,2} \geq 20°$ (see Table 1) which prohibits large exit areas and consequently low meridional flow velocities.

CONCLUSIONS

A novel design method for the impellers of centrifugal fans was developed and successfully tested. The design method consists of seven simple correlations for geometrical parameters or flow quantities. In terms of simplicity and quickness the method compares well to classic methods such as the slip theory by Pfleiderer. However, since the novel correlations have been obtained by application of a comprehensive optimization tool, the accuracy in terms of meeting the design target is better than the accuracy of classic methods. Moreover, it was found that the efficiency of the designs obtained with this new method is always superior over designs via classic methods. This holds true for all design points of typical centrifugal fans but is more pronounced for design points requiring high blade loading. Corrections may become necessary if the characteristic Reynolds number and secondary parameters (e.g. inflow conditions, size of gaps) differ substantially from the assumptions on which the design correlations are based on.

ACKNOWLEDGMENT

Part of this work was funded by the German Ministry for Economic Affairs and Energy (BMWi), the German Federation of Industrial Research Associations (AiF) and the Research Association for Air and Drying Technology (FLT) under the project number 18084.

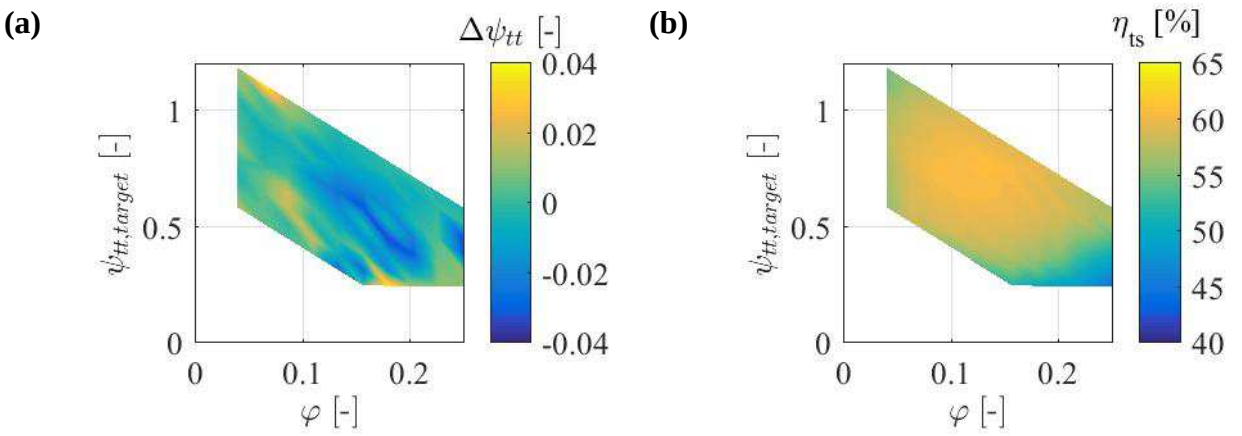

Figure 5: Impellers designed by means of the novel design correlations: (a) Deviation of actual and targeted pressure coefficient ($\Delta\psi_{tt} = \psi_{tt,actual} - \psi_{tt,target}$); (b) Total-to-static efficiency; (one correction step for μ according to Equation (14))

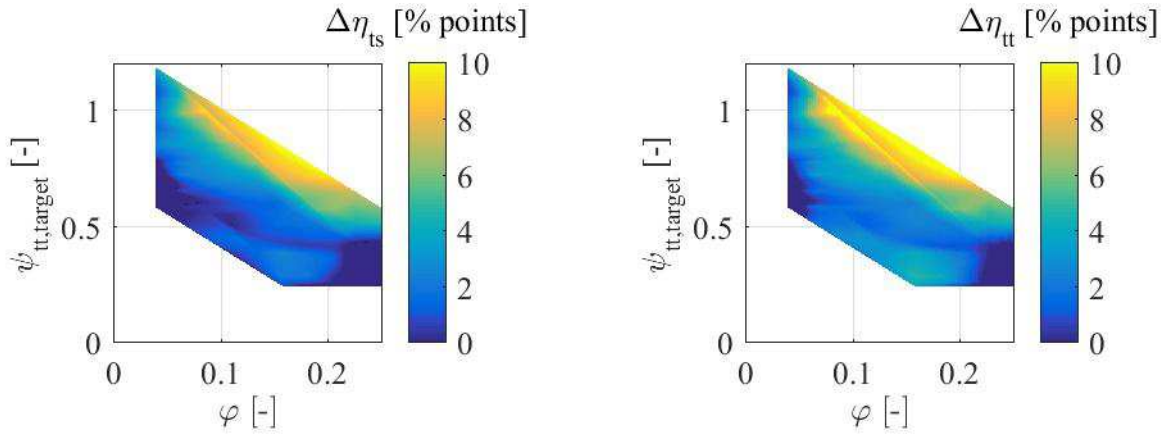

Figure 6: Difference of efficiency between impellers designed with the novel design correlations and the classic Pfleiderer method ($\Delta\eta_{tt/ts} = \eta_{tt/ts,actual} - \eta_{tt/ts,Pfleiderer}$)

REFERENCES

[1] Pfleiderer, C., 1961, Die Kreiselpumpe für Flüssigkeiten und Gase, *Springer Verlag*, Berlin-Heidelberg.

[2] Pfleiderer, C., Petermann, H., 1991, Strömungsmaschinen, *Springer-Verlag*, Berlin, Germany.

[3] Eck, B., 2003, Ventilatoren, *Springer Verlag*, Berlin, Germany.

[4] Carolus, T., 2012, Ventilatoren - Aerodynamischer Entwurf, Schallvorhersage, Konstruktion, *Springer Vieweg*, Wiesbaden, Germany.

[5] Bommes, L., Fricke, J., Grundmann, R., 2003, Ventilatoren, *Vulkan Verlag*, Essen.

[6] Pohl, C., 2001, "Schaufelformen bei Industrie-Radialventilatoren", *Proc. VDI Ventilatortagung*, Braunschweig, VDI Verlag.

[7] Lee, Y.-T., Ahuja, V., Hosangadi, A., Slipper, M. E., Mulvihill, L. P., Birkbeck, R., Coleman, R., 2011, "Impeller Design of a Centrifugal Fan with Blade Optimization", *INternational Journal of Rotating Machinery*, Article ID 537824, p. 16.

[8] Demeulenaere, A., Ligout, A., Dijkers, R., Purwanto, A., Hirsch, C., Visser, F., 2005, "Design and Optimization of an Industrial Pump: Application of Genetic Algorithms and Neural Networks", *Proc. ASME Fluids Engineering Division Summer Meeting & Exhibition 2005*, Houston, TX.

[9] Pierret, S., Hirsch, C., 2003, An Integrated Optimization System for Turbomachinery Blade Shape Design, *Defense Technical Information Center*, Brussels, Belgium.
[10] Hildebrandt, T., Starke, A., Ruck, G., 2010, "Leistung- und Effizienzsteigerung einer Diagonallüfterstufe: Von der CFD basierten Optimierung mit FINE™/Turbo bis zur Serieneinführung", *Proc. VDI Ventilatoren 2010,* Braunschweig, Germany.
[11] Bamberger, K., Belz, J., Carolus, T., Nelles, O., 2016, "Aerodynamic Optimization of Centrifugal Fans Using CFD-Trained Meta-Models", *Proc. International Symposium on Transport Phenomena and Dynamics of Rotating Machinery (ISROMAC) 2016*, Honolulu, Hawaii, USA.
[12] Dixon, S. L., Hall, C. A., 2010, Fluid Mechanics and Thermodynamics of Turbomachinery - Sixth Edition, *Butterworth Heinemann*, Oxford.
[13] Santner, T., Williams, B., Notz., W., 2003, The design and analysis of computer experiments, *Springer Science & Business Media*.
[14] Ebert, T., Fischer, T., Belz, J., Heinz, T. O., Kampmann, G., Nelles, O., 2015, "Extended Deterministic Local Search Algorithm for Maximin Latin Hypercube Designs", *Proc. IEEE Symposium on Computational Intelligence in Control and Automation*.
[15] Nelles, O., 2006, "Axes-Oblique Partitioning Strategies for Local Model Networks", *Proc. International Symposium on Intelligent Control*.
[16] Marquardt, 1963, "An Algorithm for Least-Squares Estimation of Nonlinear Parameters", *SIAM Journal of Applied Mathematics*, 11, pp. 431-441.
[17] Thévenin, D., Janiga, G., 2008, Optimization and Computational Fluid Dynamics, *Springer Verlag GmbH*, Heidelberg, Germany.
[18] Nelder, J. A., Mead, R., 1965, "A Simplex Method for Function Minimization", *Computer Journal*, 7, pp. 308-313.
[19] Bamberger, K., 2015, "Aerodynamic Optimization of Low-Pressure Axial Fans", *PhD Thesis*, University of Siegen.